THE ASTROPHYSICAL JOURNAL, 554:725–733, 2001 June 20

THEORETICAL IMPLICATIONS FROM THE SPECTRAL EVOLUTION OF MARKARIAN 501 OBSERVED WITH *BeppoSAX*

F. TAVECCHIO,[1] L. MARASCHI,[1] E. PIAN,[2] L. CHIAPPETTI,[3] A. CELOTTI,[4] G. FOSSATI,[5] G. GHISELLINI,[1] E. PALAZZI,[6] C. M. RAITERI,[7] R. M. SAMBRUNA,[8] A. TREVES,[9] C. M. URRY,[10] M. VILLATA,[7] AND A. DJANNATI-ATAÏ[11]

Received 2000 December 11; accepted 2001 February 21

ABSTRACT

We present new *BeppoSAX* observations of the TeV-emitting blazar Mrk 501 performed in 1999 June and a homogeneous reanalysis of all the *BeppoSAX* observations during the period from 1997 April to 1999 June. Recently published TeV spectra by the Cerenko Array at Themis, which are quasi-simultaneous with the 1997 *BeppoSAX* pointings, are used to constrain further the physical parameters of the jet in 1997 April with detailed models of the X-ray and TeV components. During the 1997–1999 period, the peak frequency of the synchrotron emission moved from about 100 keV in 1997 April to 0.5 keV in 1999 June. The shift in the peak frequency appears to be correlated with the long-term luminosity decrease. We interpret the results in the framework of a homogeneous synchrotron self-Compton model, discussing the evolution of the physical parameters of the emitting region under simple assumptions for the variability model. We also compute the expected variations of the TeV flux under the same assumptions.

Subject headings: BL Lacertae objects: individual (Markarian 501) — radiation mechanisms: nonthermal — X-rays: galaxies

1. INTRODUCTION

Blazars (BL Lacerate objects and flat-spectrum radio quasars) are radio-loud active galactic nuclei characterized by a bright radio core with a flat spectrum and extreme variability at all wavelengths. The current scenario (see, e.g., Urry & Padovani 1995) assumes that the strong broadband continuum is produced in a relativistic jet pointing toward the observer: relativistic effects amplify the received flux, avoiding the Compton catastrophe implied by the extreme apparent compactness.

The discovery of TeV emission from a handful of nearby BL Lac objects (for a general account of TeV observations, see Catanese & Weekes 1999) opened a new window on the study of the physics of blazars and relativistic jets. Indeed, the observation of these extreme objects can shed light on the processes responsible for the acceleration of particles up to ultrahigh energies.

Currently, the broadband spectra of TeV blazars are generally interpreted in the framework of synchrotron self-Compton (SSC) models (see, e.g., Bloom & Marscher 1996; Ghisellini, Maraschi, & Dondi 1996; Dermer, Sturner, & Schlickeiser 1997; Mastichiadis & Kirk 1997), which assume that the radio–to–X-ray continuum originates from synchrotron emission of relativistic electrons accelerated in the jet, while the γ-ray emission is produced through inverse Compton upscattering of these photons by the same electron population. In the simplest version of this model, which considers a single homogeneous emitting region, the physical parameters can be fully constrained using a relatively small set of spectral data and the minimum variability timescale (see, e.g., Tavecchio, Maraschi, & Ghisellini 1998, hereafter T98; see also Bednarek & Protheroe 1997). Other scenarios have been invoked, in particular, hadronic models considering proton initiated cascades (e.g., Mannheim 1998; Rachen 2001) or direct synchrotron emission from high-energy protons (Aharonian 2000), but they are not considered in the present work.

Mrk 501 was the second BL Lac object detected in the TeV band (Quinn et al. 1996; Bradbury et al. 1997). Its TeV spectrum is well fitted by a power law with a high-energy exponential cutoff (see, e.g., Aharonian et al. 1999; Djannati-Ataï et al. 1999). In the spring of 1997, it exhibited a phase of very high activity and showed the most extreme X-ray/TeV flare ever recorded (Catanese et al. 1997; Pian et. al 1998). Since that time, Mrk 501 has been the target of numerous observations at all wavelengths, in particular at high energies (see, e.g., Kataoka et al. 1999; Sambruna et al. 2000).

In this paper we present a systematic analysis of the *BeppoSAX* observations of Mrk 501 in 1997 April, the period of the extreme flare, 1998 April–May, and 1999 June (the second and the third observations have been only preliminarily presented in Pian et al. 1999, 2001). Section 2 describes the observations and gives the results of the spectral analysis. In § 3 we present new spectral fits for the 1997 flare, applying the SSC model to the X-ray spectra and to the quasi-simultaneous TeV spectra recently published by Djannati-Ataï et al. (1999), and discuss the implications of the observed spectral history within a simple picture for the

[1] Osservatorio Astronomico di Brera, via Brera 28, Milano, I-2021, Italy.
[2] Osservatorio Astronomico di Trieste, via G. B. Tiepolo 11, Trieste, 34131, Italy.
[3] Instituto di Fisica Cosmica G. Occhialni, via Bassini 15, Milano, I-20133, Italy.
[4] Scuola Internazionale Superiore di Studi Avanzati, Astrophysics Sector, via Beirut 4,Trieste, I-34014, Italy.
[5] Center for Astrophysics and Space Science, University of California, San Diego, 9500 Gilman Drive, Code 0424, La Jolla, CA 92093.
[6] Instituto di Tecnologie e Studio delle Radiazioni Extraterrestri, CNR, via Gobetti 101, Bologna, I-40129, Italy.
[7] Osservatorio Astronomico di Torino, Strada Osservatorio 20, Pino Torinese, I-10025, Italy.
[8] George Mason University, Department of Physics and Astronomy, 4400 University Drive, Fairfax, VA 22030.
[9] Dipartmento di Fisica, Università dell' Insubria, Como, Italy.
[10] Space Telescope Science Institute, 3700 San Martin Drive, Baltimore, MD 21218.
[11] Astroparticle Group, PCC-College de France, Paris, France.

long-term variability. In § 4 we summarize the results and present our conclusions.

2. *BeppoSAX* OBSERVATIONS

The *BeppoSAX* scientific payload (see Boella et al. 1997 and references therein) includes four co-aligned narrow field-instruments (NFIs), namely, the Low-Energy Concentrator/Spectrometer (LECS; 0.1–10 keV), the Medium-Energy Concentrator/Spectrometers (MECS; 2–10 keV), the Phoswich Detector System (PDS; 15–200 keV), and the high pressure gas scintillation proportional counter. Here we will consider data from the first three instruments.

The journal of observations of Mrk 501 is reported in Table 1. In Figure 1 we report the All-Sky Monitor (ASM) light curve for the period from 1997 to 1999. The vertical dashed lines indicate the epochs of *BeppoSAX* pointings. It appears that there are long-term trends in the overall light curve. The 1997 observations correspond to a rather high "average" flux (where the average is taken over 10 days), but not to the peak of the long-term light curve. In the two following years, the ASM light curve shows an overall decline in the intensity, interrupted, however, by one major flare. The subsequent 1998 and 1999 *BeppoSAX* observations took place in the declining phase outside flaring periods. During the *BeppoSAX* pointings, the source does not show variations of large amplitude, $\Delta F/F < 10\%$–20%. Even during the long exposure ($\sim 4 \times 10^5$ s) of 1999 June 6 (the light curve is reported in Fig. 2), although the source was clearly variable, the amplitude did not exceed $\Delta F/F < 20\%$. Unfortunately, the relatively low count rate does not allow us to explore very short timescales (~ 1000 s), as was done by Catanese & Sambruna (2000) with *Rossi X-Ray Timing Explorer* (*RXTE*) data.

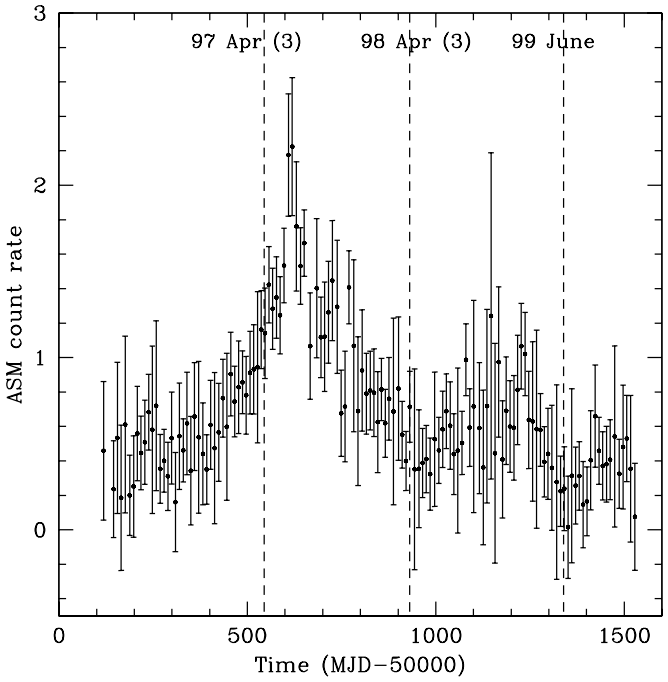

FIG. 1.—*RXTE* ASM light curve of Mrk 501. The vertical dashed lines indicate the periods of *BeppoSAX* observations whose number is reported in parentheses. These points are averaged over 10 days of measurements.

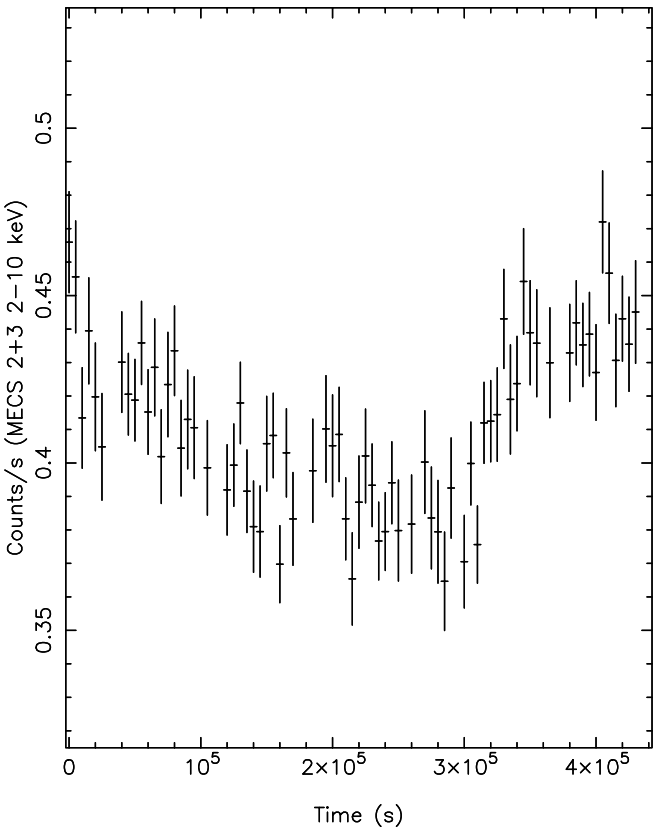

FIG. 2.—MECS light curve of Mrk 501 taken in 1999 June 6 (the bin size is 5000 s). Despite the long exposure ($\simeq 5 \times 10^4$ s), the source showed only small amplitude variations ($\sim 10\%$–20%).

2.1. *Analysis Procedure*

The data have been analyzed following the *BeppoSAX* NFI Spectral Analysis Cookbook[12] using the standard software packages XSELECT (v1.4b) and XSPEC (v10.0) and the response matrices released in 1998 November. From the cleaned and linearized event files provided by the *BeppoSAX* Scientific Data Center, we extracted the LECS and MECS spectra from circular regions centered on the source position with radii of 8′ and 4′, respectively. We used background spectra extracted from the same detector regions in blank field exposures. As discussed above, the light curves do not show variations of large amplitude. Therefore, for each observation, a single spectrum was extracted.

We jointly fitted the LECS, MECS, and PDS spectra after rebinning (using the rebinning files provided by the Scientific Data Center), allowing the two normalization factors to be free to take into account intercalibration uncertainties between the instruments (see the *SAX* Cookbook). For the LECS, we considered only data in the 0.1–4 keV energy range because of unsolved calibration problems at higher energies.

Clearly, a simple absorbed power law does not provide a good fit to the data. We also tried to fit the spectra with a power law with a cutoff at high energy, but the resulting fits are not good and we exclude the peak is due to the presence of a cutoff.

[12] Available at ftp://www.sdc.asi.it/pub/sax/doc/software_docs/saxabc_v1.2.ps.gz.

TABLE 1

BeppoSAX Data Observation Log

Date	Start Time	End Time	LECS Exposure (s)	LECS Count Rate[a] (counts s^{-1})	MECS Exposure (s)	MECS Count Rate[b] (counts s^{-1})	PDS Exposure (s)	PDS Count Rate (counts s^{-1})
1997 Apr 7.....	05:11	16:02	12724	2.13 ± 0.01	20571	3.78 ± 0.01	9280	1.94 ± 0.07
1997 Apr 11.....	05:22	16:26	12826	2.15 ± 0.01	20391	4.11 ± 0.01	9163	2.39 ± 0.07
1997 Apr 16.....	03:20	14:36	9632	3.54 ± 0.02	17125	8.61 ± 0.02	7800	8.37 ± 0.08
1998 Apr 28–29.....	8:52	02:19	13560	1.60 ± 0.01	21910	2.15 ± 0.01	9870	1.51 ± 0.06
1998 Apr 29–30.....	20:33	13:40	14660	1.90 ± 0.01	21427	2.54 ± 0.01	9660	1.86 ± 0.06
1998 May 1–2	19:02	10:38	13180	1.60 ± 0.01	19045	1.862 ± 0.01	8450	0.91 ± 0.06
1999 Jun 6–7.....	23:01	02:11	104000	0.512 ± 0.002	175400	0.420 ± 0.002	78400	0.105 ± 0.002

[a] 0.1–4 keV.

[b] 1.8–10.5 keV; 2 MECS units.

We modeled the spectral data with both the broken power-law model and the curved model introduced by Fossati et al. (2000), both with free and Galactic column densities ($N_{\rm H,Gal} = 1.73 \times 10^{20}$ cm^{-2}; Stark et al. 1992). The curved model is represented by

$$F(E) = KE^{-\Gamma_-}\left(1 + \frac{E}{E_b}\right)^{\Gamma_- - \Gamma_+} . \quad (1)$$

This expression describes a continuum, the slope (derivative) of which changes continuously with energy (frequency) between two asymptotic values, Γ_- and Γ_+. E_b represents the energy (break) around which the change between the two asymptotic slopes occurs. The model is implemented in the fitting procedure in such a way that the values of the local slope at two fixed energies E_1 and E_2 can be derived, or alternatively, one can derive the energies at which the local slope assumes two given values Γ_1 and Γ_2.

The adopted parameterization of the curved model is very useful: in particular, it allows one to find the energy at which the νF_ν spectrum peaks ($E_{\rm peak}$), defined as the energy at which the local slope of the photon spectrum is $\Gamma = 2$. For further details on the curved model, we refer to the paper of Fossati et al. (2000). The asymptotic indices can be derived a posteriori but may not have great meaning if they refer to energy ranges outside the observed band.

2.2. *Results*

The results of the spectral fits are reported in Tables 2 and 3 for the broken power-law and the curved model, respectively. For the curved model, we report the photon indices at 0.1 and 10 keV and the break energy E_b. These are the fitted parameters.

The value of χ^2 favors the curved model with respect to the broken power-law model (both for fixed and free $N_{\rm H}$),

TABLE 2

FITS TO *BeppoSAX* DATA (LECS + MECS + PDS) WITH THE BROKEN POWER-LAW MODEL

Observation Date	Γ_1 [a]	E_b [b] (keV)	Γ_2 [c]	$N_{\rm H}$ ($\times 10^{20}$ cm^{-2})	χ^2/degrees of freedom
97 Apr 7	$1.58^{1.67}_{1.48}$	$1.17^{1.35}_{1.06}$	$1.92^{1.94}_{1.91}$	$2.02^{2.29}_{1.75}$	180.98/184
97 Apr 7	$1.48^{1.51}_{1.44}$	$1.11^{1.20}_{1.03}$	$1.93^{1.94}_{1.91}$	Galactic	184.25/185
97 Apr 11	$1.64^{1.76}_{1.51}$	$1.10^{1.94}_{0.87}$	$1.81^{1.83}_{1.80}$	$2.21^{2.54}_{1.89}$	188.92/186
97 Apr 11	$1.46^{1.50}_{1.39}$	$0.92^{1.06}_{0.78}$	$1.81^{1.82}_{1.80}$	Galactic	195.03/187
97 Apr 16	$1.56^{1.57}_{1.54}$	$6.00^{6.36}_{5.62}$	$1.82^{1.85}_{1.80}$	$2.55^{2.67}_{2.44}$	325.56/289
97 Apr 16	$1.47^{1.48}_{1.45}$	$4.28^{4.65}_{3.87}$	$1.76^{1.79}_{1.73}$	Galactic	471.97/290
98 Apr 28	$1.56^{1.64}_{1.46}$	$1.24^{1.44}_{1.09}$	$1.84^{1.86}_{1.83}$	$1.92^{2.18}_{1.65}$	216.38/188
98 Apr 28	$1.49^{1.53}_{1.45}$	$1.18^{1.30}_{1.07}$	$1.84^{1.86}_{1.83}$	Galactic	217.73/189
98 Apr 29	$1.59^{1.66}_{1.50}$	$1.51^{2.02}_{1.29}$	$1.85^{1.86}_{1.83}$	$2.07^{2.32}_{1.80}$	203.29/188
98 Apr 29	$1.48^{1.51}_{1.45}$	$1.32^{1.45}_{1.22}$	$1.84^{1.86}_{1.83}$	Galactic	208.07/189
98 May 1	$1.77^{1.80}_{1.73}$	$2.61^{2.88}_{2.33}$	$2.07^{2.10}_{2.04}$	$2.35^{2.53}_{2.19}$	233.28/188
98 May 1	$1.62^{1.64}_{1.59}$	$1.89^{2.13}_{1.61}$	$2.02^{2.04}_{2.00}$	Galactic	265.37/189
99 Jun 6	$2.13^{2.20}_{2.07}$	$1.28^{1.54}_{1.16}$	$2.44^{2.46}_{2.43}$	$2.40^{2.58}_{2.23}$	204.68/188
99 Jun 6	$1.89^{1.91}_{1.86}$	$1.07^{1.12}_{1.01}$	$2.44^{2.45}_{2.42}$	Galactic	254.81/189

NOTE.—Errors (given as upper and lower limits) are quoted at the 90% confidence level for one parameter of interest.

[a] Photon index at 1 keV.

[b] Break Enrgy.

[c] Photon index at 2 keV.

TABLE 3

FITS TO *BeppoSAX* DATA (LECS + MECS + PDS) WITH THE CURVED MODEL

Observation Date	$\Gamma_{0.1}$ [a]	E_b [b] (keV)	Γ_{10} [c]	$N_{\rm H}$ ($\times 10^{20}$ cm^{-2})	χ^2/degrees of freedom
1997 Apr 7	$0.86^{1.47}_{0.0}$	$0.21^{0.86}_{0.0}$	$2.00^{2.01}_{1.96}$	$1.76^{2.20}_{1.30}$	181.87/184
1997 Apr 7	$0.79^{1.1}_{0.0}$	$0.18^{0.41}_{0.0}$	$2.00^{2.01}_{1.96}$	Galactic	181.86/185
1997 Apr 11	$0.75^{1.69}_{0.23}$	$0.01^{1.23}_{0.0}$	$1.84^{1.86}_{1.82}$	$2.02^{2.38}_{1.69}$	190.92/186
1997 Apr 11	$0.32^{0.82}_{0.17}$	$0.01^{0.1}_{0.0}$	$1.85^{1.86}_{1.83}$	Galactic	192.99/187
1997 Apr 16	$1.35^{1.42}_{1.28}$	$4.54^{6.99}_{2.95}$	$1.73^{1.75}_{1.72}$	$1.99^{2.18}_{1.78}$	280.29/289
1997 Apr 16	$1.26^{1.30}_{1.22}$	$2.97^{3.88}_{2.23}$	$1.74^{1.75}_{1.72}$	Galactic	284.53/290
1998 Apr 28	$1.66^{1.72}_{1.58}$	$16.27^{61.33}_{4.65}$	$2.01^{2.06}_{1.97}$	$2.26^{2.46}_{2.04}$	197.66/188
1998 Apr 28	$1.31^{1.44}_{1.06}$	$0.89^{2.31}_{0.30}$	$1.94^{1.99}_{1.90}$	Galactic	205.88/189
1998 Apr 29	$1.51^{1.63}_{1.22}$	$2.90^{9.23}_{0.74}$	$1.97^{2.03}_{1.92}$	$2.07^{2.33}_{1.71}$	192.24/188
1998 Apr 29	$1.26^{1.37}_{1.09}$	$0.92^{1.75}_{0.45}$	$1.94^{1.99}_{1.91}$	Galactic	194.77/189
1998 May 1	$1.48^{1.61}_{1.23}$	$2.81^{7.23}_{1.1}$	$2.22^{2.31}_{2.15}$	$1.89^{2.16}_{1.56}$	196.94/188
1998 May 1	$1.38^{1.46}_{1.27}$	$1.94^{3.44}_{1.09}$	$2.20^{2.27}_{2.14}$	Galactic	197.0/189
1999 Jun 6.....	$1.81^{2.02}_{1.40}$	$0.78^{1.88}_{0.29}$	$2.55^{2.60}_{2.52}$	$2.19^{2.42}_{1.92}$	193.84/188
1999 Jun 6.....	$1.00^{1.28}_{0.48}$	$0.17^{0.32}_{0.06}$	$2.53^{2.56}_{2.50}$	Galactic	200.56/189

NOTE.—Errors (given as upper and lower limits) are quoted at the 90% confidence level for one parameter of interest.

[a] Photon index at 0.1 keV.

[b] Break energy.

[c] Photon index at 10 keV.

except for the cases of 1997 April 7 and 11, for which the two models are equivalent. Note also that the curved model with free absorption yields N_H values consistent with the Galactic column, while the broken power-law model yields systematically higher values of N_H. These higher values probably mimic the intrinsically curved shape of the spectrum. We conclude that the continuously curved model is a better representation of the data and that no intrinsic absorption is required.

2.2.1. *Correlations between Spectral Parameters*

Although our data are snapshots distributed with large separations over 2 yr, the spectral behavior appears to be extremely "regular." The unfolded vF_v spectra, obtained from the best fits with the curved model, are shown in Figure 3 for four epochs that differ significantly in total flux, i.e., 1997 April 16, 1998 April 29, and May 1, and 1999 June. It can be checked from the tables that spectra with similar fluxes have very similar shapes; these are omitted from the figure for clarity. This series strongly suggests that the spectral evolution from the highest flaring state to the lowest 1999 state consists of a systematic steepening of the spectrum that sets in at progressively lower energies with little variation in flux or spectral shape at the low-energy end.

We can characterize the spectral evolution by the spectral slope Γ_{10} at an energy of 10 keV or by the peak energy of the vF_v plot as defined in the previous subsection. The values of the peak energy in the $vF(v)$ plot, E_{peak} (calculated for Galactic column density using the procedure described in the previous section), together with the fluxes in the soft (0.1–2 keV), medium (2–10 keV), and hard bands (10–100 keV), are reported in Table 4. For five epochs, the best-fit value and the lower bound of E_{peak} can be derived, while the upper bound cannot be constrained. In Figures 4 and 5, we plot the two parameters versus the total flux (0.1–100 keV). In the case of Γ_{10}, the anticorrelation is very strong ($r = -0.93$). The significance of this correlation is confirmed by the nonparametric Spearman's test, which gives a chance probability of less than 3×10^{-2}. In the case of E_{peak}, unfortunately, five of seven cases result in an ill-defined value because the energy distributions do not "converge" clearly, and only a lower limit can be derived.

1. Γ_{10} *versus* F_{2-10} keV.—A least-squares analysis gives the relation $\Gamma_{10} = 2.2 - 0.7(\pm 0.1) \log F_{2-10}$ keV. A similar

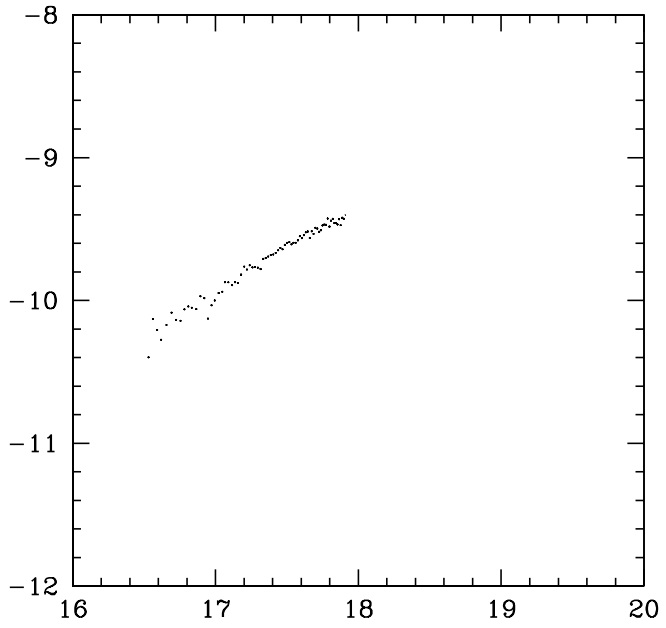

FIG. 3.—History of the X-ray spectrum of Mrk 501 (deconvolved spectra fitted with the curved model). *From top to bottom*: 1997 April 16, 1998 April 29, 1998 May 1, and 1999 June 6.

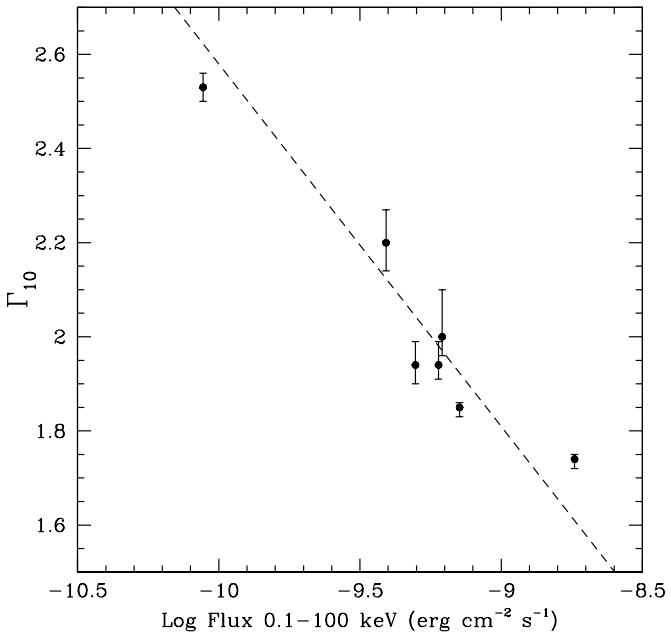

FIG. 4.—Photon index at 10 keV vs. total (0.1–100 keV) X-ray flux for the different epochs. The dashed line shows the least-squares fit reported in the text.

TABLE 4

X-RAY FLUX IN THE SOFT, MEDIUM, AND HARD BANDS AND THE BEST-FIT VALUE

Observation	$F_{0.1-2}$ keV ($\times 10^{-10}$ ergs cm^{-2} s^{-1})	F_{2-10} keV ($\times 10^{-10}$ ergs cm^{-2} s^{-1})	F_{10-100} keV ($\times 10^{-10}$ ergs cm^{-2} s^{-1})	E_{peak}[a] (keV)
1997 Apr 7	1.42	2.14	2.62	100^{*}_{8}
1997 Apr 11	1.421	2.39	3.32	100^{*}_{50}
1997 Apr 16	2.07	5.22	10.9	100^{*}_{86}
1998 Apr 28	1.05	1.76	2.16	100^{*}_{11}
1998 Apr 29	1.22	2.08	2.70	$45.8^{100}_{11.5}$
1998 May 1	1.06	1.46	1.39	$3.2^{3.1}_{3.7}$
1999 Jun 6	0.42	0.30	0.16	$0.36^{0.04}_{0.50}$

NOTE.—The asterisks denote unconstrained values.

[a] The 90% error range for the peak energy was determined with the curved model described in the text.

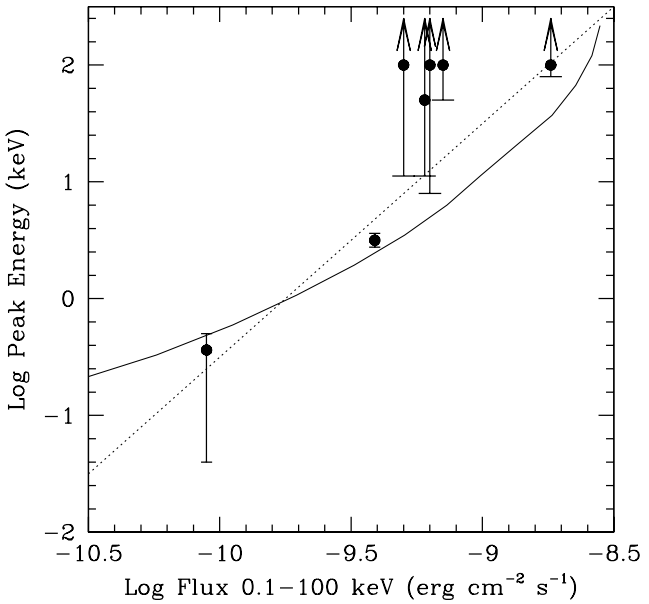

FIG. 5.—Energy of the synchrotron peak (obtained by fitting the data with the curved model described in the text) vs. text. The solid line show the $E_{\rm peak}$-F relations predicted by the simple picture described in the text, calculated for two different energy bands. Clearly, the slope depends on the flux.

correlation between the flux and the high-energy photon index has been found by analyzing the observations of Mrk 421 (Fossati et al. 2000). This *hardening-brightening* behavior seems to be quite general in blazars (see, e.g., Ulrich, Maraschi, & Urry 1997), although only recently has it been confirmed in this detail on long timescales.

2. $E_{\rm peak}$ *versus* $F_{0.1-100}$ keV.—Although the determination of the relation between the synchrotron peak and flux is limited by the large number of lower limits, the data in Figure 5 suggest a relation of the form $E \propto F^n$, with $n \gtrsim 2$. In any case, the slope of this relation seems to be definitely larger than the exponent 0.55 found in a similar analysis of Mrk 421 (Fossati et al. 2000).

3. INTERPRETATION

We will discuss the results in light of the simplest, but widely adopted, theoretical framework: the "one-zone" SSC model. Specifically, we adopt the version described and used by T98 and Maraschi et al. (1999).

Briefly, the observed radiation is assumed to be produced in a spherical region (blob) with radius R, moving at relativistic velocity βc [which corresponds to a bulk Lorentz factor $\Gamma = (1 - \beta^2)^{-1/2}$], at a small angle θ with respect to the line of sight. The relevant relativistic effects are described by the relativistic Doppler factor $\delta = \Gamma^{-1}(1 - \beta \cos \theta)^{-1}$, with $\delta \simeq \Gamma$ for $\theta \simeq 1/\Gamma$. The blob is filled with relativistic electrons and a tangled magnetic field with intensity B. The electron distribution is described by the law

$$N(\gamma) = K\gamma^{-n_1}\left(1 + \frac{\gamma}{\gamma_b}\right)^{n_1 - n_2} \exp\left(\frac{-\gamma}{\gamma_{\rm max}}\right), \qquad (2)$$

where K is a normalization factor, γ_b is the break Lorentz factor, and n_1 and n_2 are the spectral indices below and above the break, respectively. This particular form for the distribution function has been assumed on a purely phenomenological basis in order to describe the curved shape of the spectral energy distribution (SED). In other models, the electron energy distribution function is determined from a kinetic equation (Ghisellini et al. 1998; Kirk, Rieger, & Mastichiadis 1998). The inverse Compton emission is calculated using the full Klein-Nishina (KN) emissivity given by Jones (1968).

3.1. *Spectral Models for the 1997–1999 SEDs*

3.1.1. *1997 Data*

Several groups obtained good quality TeV spectra (Aharonian et al. 1999; Djannati-Ataï et al. 1999; Krennrich et al. 1999) at epochs close to the 1997 flare observed by *BeppoSAX*. In particular, the Cerenko Array at Themis (CAT) spectra that are nearly simultaneous with the *BeppoSAX* observations of 1997 April 7 and 16 are discussed in detail by Djannati-Ataï et al (1999). For the large flare of April 16, given the high flux level, it was possible to obtain a good quality TeV spectrum using a single observation that partially overlaps the *BeppoSAX* observation. On April 7, Mrk 501 was less bright, and the TeV spectrum was obtained by summing different observations with similar TeV fluxes and hardness ratios (for more details, we refer to Djannati-Ataï et al 1999). These spectra could not be included in the fits published by Pian et al. (1998) since they were not available at that time. We therefore rediscuss the emission models here using the old *BeppoSAX* data unfolded with the curved model and the quasi-simultaneous TeV spectra obtained by Djannati-Ataï et al (1999).

SSC models for the observed SEDs were computed as described above. The values of the fitted physical quantities are reported in Table 5. In the calculation, we have assumed a typical radius of the emitting region of $R \sim 10^{15}$ cm and a Doppler factor $\delta \simeq 10$. With these choices, the observed minimum variability timescale is on the order of $R/c\delta \simeq 1$ *h*. Recently, Catanese & Sambruna (2000) have reported the observation with *RXTE* of a very rapid flare event during 1999 May with an increase in the 2–10 keV flux of 60% in less than 200 s. The size of the emitting source corresponds

TABLE 5

VALUES OF THE PHYSICAL PARAMETERS USED FOR THE SSC MODEL

Observation	R_{15} (cm)	B (G)	δ	$\gamma_{\rm break}$	K (cm^{-3})	n_1	n_2
1997 April 7	1.9	0.32	10	1.1×10^5	750	1.5	3
1997 April 16	1.9	0.32	10	7×10^5	10^3	1.55	3
1997 Apr 16 + Absorption.....	1.9	0.32	10	10^6	8×10^2	1.55	3
1998 Apr 29	1.9	0.32	10	3×10^5	3×10^2	1.5	3.3
1999 Jun	1.9	0.32	10	1.06×10^5	3.5×10^2	1.5	4.3

to $\sim 10^{14}$ cm for $\delta = 10$, about 10 times smaller than the dimension used in our model fits. Such an event is exceptional, however, within the extensive monitoring of the source since 1997 in the X-ray and TeV bands. Therefore, we feel justified in assuming that the emission region is usually less extreme in size and/or Doppler factor than during the above flare. In Figure 6 we show the quasi-simultaneous SEDs for the two epochs constructed with the X-ray/TeV unfolded spectra.

The inverse Compton (IC) peak occurs in the KN regime, and therefore its energy is mainly determined by the value of γ_b. In fact, as shown in T98, the IC peak frequency can be estimated as $E_{\rm IC} = Am_e c^2 \gamma_b$, where the factor $A < 1$ depends on the spectral shape.

The X-ray data set only a lower limit to the frequency ν_s of the synchrotron peak, $\nu_s > 10^{20}$ Hz, but the EGRET upper limit reported by Catanese et al. (1997) constrains it to fall below $\sim 10^{21}$ Hz. We fitted the flare data assuming a synchrotron peak frequency of $\sim 10^{20}$ Hz. Since, in the KN regime, γ_b is univocally determined by the IC peak, the uncertainty in the position of ν_s ($\propto B\gamma_b^2\,\delta$) mainly affects the determination of the magnetic field B; in this sense, the value of B derived from our fits should be considered a lower limit.

Absorption of TeV photons by the intergalactic infrared background (IRB; see, e.g., Konopelko et al. 1999; Guy et al. 2000; Krawczynski et al. 2000) could be important in determining or contributing to the steepening of the TeV spectra at very high energies. We considered the effect of a possible intervening absorption by the IRB. Taking absorption into account modifies the intrinsic spectra in the sense that a higher value of γ_b is required (see Table 5). Stecker & de Jager (1998) proposed a simple polynomial expression for the pair-production optical depth for γ-ray photons. Because of the large uncertainties involved, they discuss two models corresponding to the high and low bounds on the actual IRB flux. Adopting their prescriptions for the *low model*, we found that γ_b increases from 7×10^6 to 10^7 for the spectrum of April 16. In this work we are mainly interested in the study of the *evolution* of the physical quantities in the jet. Since γ-ray absorption is still uncertain and since it becomes important only above 2–3 TeV, where there are good data only for the high state, we neglect it in the following discussion.

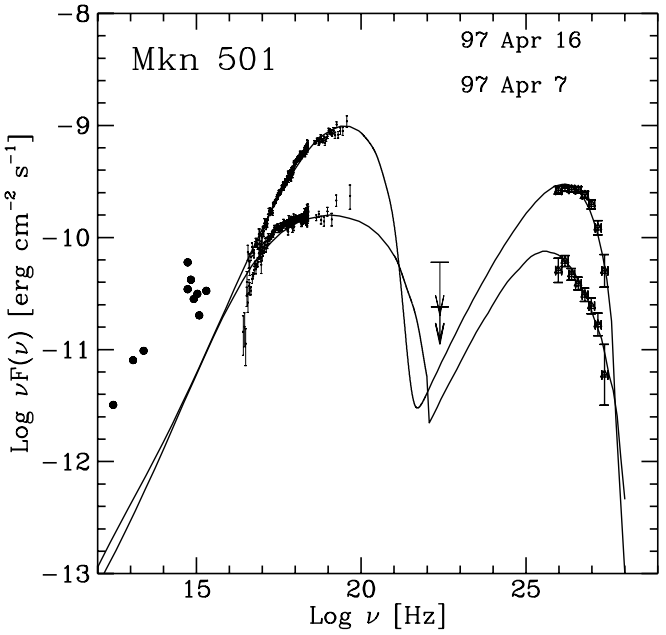

FIG. 6.—Overall SED of Mrk 501 in 1997 April. The CAT TeV spectra are from Djannati-Ataï et al. (1999). The solid line is the spectrum calculated with the homogeneous SSC model described in the text.

In the earlier paper of Pian et al. (1998), it was suggested that the flare observed in 1997 could be due to an increase in the maximum Lorentz factor of emitting particles. The recently published TeV spectra demonstrate that the IC peak also shifts to higher energy during the flare (see Djannati-Ataï et al. 1999; Aharonian et al. 2001), as predicted by the Pian et al. interpretation. The transition between the two states of April 7 and 16 can be accounted for by an increase of a factor of 7 in γ_b with almost constant values of δ, R, and B (see Table 5).

3.1.2. *1997–1999 Data*

From the *RXTE* ASM light curve in Figure 1, it is clear that our 1997–1999 set of data does not trace a truly continuous evolution of a single flaring event given that the observations are separated by states of stronger activity. Moreover, as shown by Sambruna et al. (2000), the spectrum can vary on very short timescales. However, the correlations that we found between the high-energy spectral index and flux and between the synchrotron peak and flux (shown in § 2) suggest that the underlying mechanisms responsible for the variability are somehow "repetitive." This motivates an analysis in which the observed variability is reproduced by changes in only a few parameters while the other parameters characterizing the emitting region are almost stationary. In the widely adopted shock-in-jet picture (see, e.g., Kirk et al. 1998), this could correspond to a situation in which one of the parameters specifying the particle acceleration (e.g., the acceleration timescale) varies, while the structure of the shock remains almost stationary.

The fits of the two states of 1997 discussed above are consistent with the picture in which the key parameter regulating the variability is γ_b. This interpretation is also consistent with the observed relation between $E_{\rm peak}$, the energy of the synchrotron peak, and the flux, a relation of the form $E_{\rm peak} \propto L_s^2$ (indicated by the dotted line in Fig. 5). In fact, this relation can be easily reproduced in a simple picture in which the physical quantities in the emitting region are almost constant and in which only the Lorentz factor γ_b of electrons emitting at the synchrotron peak varies. Indeed, in that case, the synchrotron peak frequency will be $\nu_p \propto \gamma_b^2$, while the synchrotron luminosity can be written as $L_s \propto \gamma_b^{3-n}$, where n is the index of the assumed power-law electron energy distribution. Usually for blazars, $n \simeq 2$, and one naturally finds $\nu_p \propto L_s^2$. The relation actually observed is more complex, however, depending on the band in which the luminosity is evaluated (see below).

Starting from the set of parameters used to fit the 1997 data, we tried to reproduce the observed SEDs and correlations by varying γ_b only. The aim of the following analysis is not to obtain very precise fits to the SEDs but rather to study how it is possible to reproduce the observed spectral behavior and correlations with a simple unifying picture without entering in detail into the spectral fit. In Figure 7 we report the series of SEDs calculated with the adopted assumptions. The highest state corresponds to the detailed fit discussed above for 1997 April 16. Given that the spectral

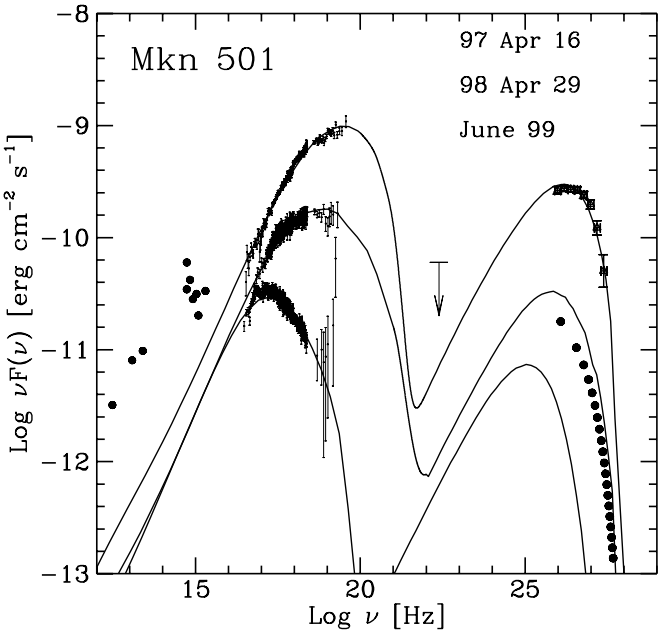

FIG. 7.—Overall SED of Mrk 501 of 1997 April 16, 1998 April 29, and 1999 June. The solid line is the spectrum calculated with the homogeneous SSC model described in the text. The filled circles are from the HEGRA 1998–1999 data (from Aharonian et al. 2001).

states observed during the three different pointings in 1998 are very similar, here we use only the April 29 spectrum. We also show (*filled circles*) the average TeV spectrum observed by the High-Energy Gamma-Ray Astronomy (HEGRA) instrument during the 1998–1999 period reported by Aharonian et al. (2001).

3.2. *Variability Correlations*

As shown above, the spectral variability of Mrk 501 on long timescales can be explained by a simple picture in which only γ_b varies. It is then possible and instructive to calculate the expected correlations between the frequency of the synchrotron peak and the X-ray flux and between the X-ray and TeV fluxes for this schematic case.

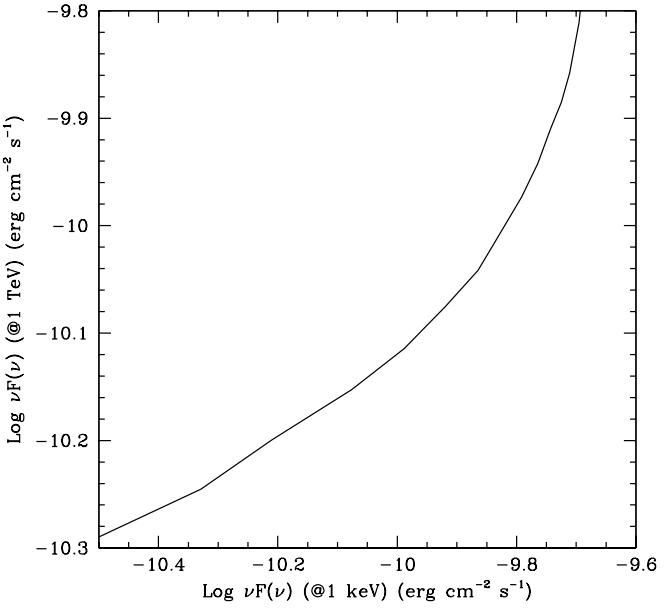

FIG. 8.—X-ray/TeV flux correlation expected for the picture presented in the text

Figure 5 shows the relation between the X-ray flux and the position of the synchrotron peak predicted by our assumptions (*solid line*). The slope of the relation depends on the position of the peak, being steeper when the peak is at higher energies. The reason for the change of the slope is that we are evaluating the flux in a limited energy band (0.1–100 keV). When the peak of the synchrotron component moves into the band from below, a small change in the position of the peak causes a large variation of the flux, and hence the relation will be quite flat. Once the peak is within the selected energy band, the increase of flux is less rapid, and eventually it stops when the peak reaches the upper limit of the band and moves out: in this region, the $E_{\rm peak}$-F relation will be very steep. We note that the rather flat correlation found in Mrk 421 by Fossati et al. (2000) is consistent with this general picture since, in the latter source, the peak was located at $\sim$1 keV, thus close to the lower limit of the observing band. More observations of sources with large flux variations, in principle, could test this hypothesis.

The broadband spectral models also show that the position of the TeV spectral peak varies with the flux level. Therefore (assuming a constant spectral shape), we expect to observe a spectral softening in the TeV range when the source flux decreases. Such behavior is in fact shown by the analysis of the CAT group (Djannati-Ataï et al. 1999) of the 1997 data, and it has been recently confirmed with HEGRA data (Aharonian et al. 2001) comparing the bright 1997 spectrum with the weaker 1998–1999 state.

From Figure 7, it appears that the IC peak shifts in frequency *less* than the corresponding synchrotron peak. This can be naturally interpreted as being due to the KN limit in which the IC peak frequency depends quasi-linearly on γ_b (see, e.g., T98), while the synchrotron peak frequency always depends on γ_b^2. This effect has to be taken into account in computing the expected relation between the X-ray flux and the TeV fluxes. In Figure 8 we show an example of the correlation for the X-ray flux at 1 keV and the TeV flux at 1 TeV calculated using the physical parameters adopted for the fit of 1997 April 16 and varying γ_b in the 10^5–10^7 range. The slope of the correlation is different at different flux levels, being steeper at higher fluxes. At low fluxes [$\nu F_\nu(1\ {\rm keV}) \simeq 10^{-10}$ ergs cm^{-2} s^{-1}], the relation is almost linear, while for higher fluxes, the relation is quadratic or even steeper. Note that the exact relation depends also on the spectral shape of the two peaks. Using pointed *RXTE* observations and HEGRA data, Krawczynski et al. (2000) found a good agreement with a quadratic relation during the 1997 flare epoch that was consistent with the slope of our relation at high fluxes. Observations at lower flux levels should show a linear correlation.

4. DISCUSSION AND CONCLUSIONS

We have presented *BeppoSAX* spectra of Mrk 501 taken at different intensities and spectral states during the 1997–1999 period. The data show a clear correlation between the spectral shape and the total flux, which holds over the whole period; in particular, we found a well-defined correlation between the spectral index at 10 keV and the flux and an indication of a steep correlation between the energy of the synchrotron peak and the flux.

For the high and low spectral states observed in 1997, using quasi-simultaneous TeV spectra obtained by the CAT group, we constructed the overall SEDs and reproduced them with a homogeneous SSC model varying only γ_b, obtaining a robust estimate of the physical quantities in the jet.

Using the full set of X-ray spectra, we tried to reproduce the observed spectral variations by varying only a few parameters. In particular, our analysis suggests that the observed spectral evolution can be accounted for by the variation of the peak Lorentz factor of the electron energy distribution. Adopting this simple picture, we compute the expected correlations between $E_{\rm peak}$ and the X-ray flux and between the X-ray and TeV fluxes. We show that, depending on the position of the peaks with respect to the fixed energy range used to estimate the flux, the correlations have different slopes in different regimes.

The phenomenology discussed above, and in particular the regularity shown by the spectral evolution, suggests that the radiation is produced by a region whose main physical quantities (size, magnetic field, Lorentz factor) remain on average almost constant. In this framework, the variations of γ_b can be interpreted as being due to changes the acceleration process. In the widely discussed diffusive shock acceleration model (see, e.g., Kirk et al. 1998), in which $\gamma_{\rm max}$ is determined by the balance between the cooling and acceleration processes, variations in the structure of the shock (e.g., the energy spectrum of the turbulence) could produce variations in the acceleration timescale, which then could be responsible for the variation in the value of γ_b. In this way, it is possible to account for large variations close to the peak, as observed, while at lower frequencies, the variations present a small amplitude, being diluted by a "bath" of lower energy electrons.

We thank the *BeppoSAX* Scientific Data Center for providing us with the cleaned data.

REFERENCES

Aharonian, F. A. 2000, NewA, 5, 377
Aharonian, F. A., et al. 1999, A&A, 349, 11
———. 2001, ApJ, 546, 898
Bednarek, W., & Protheroe, R. J. 1997, MNRAS, 292, 646
Bloom, S. D., & Marscher, A. P. 1996, ApJ, 461, 657
Boella, G., Butler, R. C., Perola, G. C., Piro, L., Scarsi, L., & Bleeker, J. A. M. 1997, A&AS, 122, 299
Bradbury, S. M., et al. 1997, A&A, 320, L5
Catanese, M., et al. 1997, ApJ, 487, L143
Catanese, M., & Sambruna, R. M. 2000, ApJ, 534, L39
Catanese, M., & Weekes, T. C. 1999, PASP, 111, 1193
Dermer, C. D., Sturner, S. J., & Schlickeiser, R. 1997, ApJS, 109, 103
Djannati-Ataï, A., et al. 1999, A&A, 350, 17
Fossati, G., et al. 2000, ApJ, 541, 166
Ghisellini, G., Celotti, A., Fossati, G., Maraschi, L., & Comastri, A. 1998, MNRAS, 301, 451
Ghisellini, G., Maraschi, L., & Dondi, L. 1996, A&AS, 120, 503
Guy, J., Renault, C., Aharonian, F. A., Rivoal, M., & Tavernet, J.-P. 2000, A&A, 359, 419
Jones, F. C. 1968, Phys. Rev., 167, 1159
Kataoka, J., et al. 1999, ApJ, 514, 138
Kirk, J. G., Rieger, F. M., & Mastichiadis, A. 1998, A&A, 333, 452
Konopelko, A. K., Kirk, J. G., Stecker, F. W., & Mastichiadis, A. 1999, ApJ, 518, L13
Krawczynski, H., Coppi, P. S., Maccarone, T., & Aharonian, F. A. 2000, A&A, 353, 97
Krennrich, F., et al. 1999, ApJ, 511, 149
Mannheim, K. 1998, Science, 279, 684
Maraschi, L., et al. 1999, ApJ, 526, L81
Mastichiadis, A., & Kirk, J. G. 1997, A&A, 320, 19
Pian, E., et al. 1998, ApJ, 492, L17
———. 1999, in ASP Conf. Ser. 159, BL Lac Phenomenon, ed. L. Takalo (San Francisco: ASP), 180
———. 2001, Astrophys. Lett. Commun., in press
Quinn, J., et al. 1996, ApJ, 456, L83
Rachen, J. P. 2001, in AIP Conf. Roc 558, High Energy Gamma Ray Astronomy, ed. F. A. Aharonian & H. J. Völk (Woodbury: AIP) (astro-ph/0010289)
Sambruna, R. M., et al. 2000, ApJ, 538, 127
Stark, A., Gammie, C. F., Wilson, R. W., Bally, J., Linke, R. A., Heiles, C., & Hurwitz, M. 1992, ApJS, 79, 77
Stecker, F. W., & de Jager, O. C. 1998, A&A, 334, L85
Tavecchio, F., Maraschi, L., & Ghisellini, G. 1998, ApJ, 509, 608 (T98)
Ulrich, M., Maraschi, L., & Urry, C. M. 1997, ARA&A, 35, 445
Urry, C. M., & Padovani, P. 1995, PASP, 107, 803